

Research Radar Facilities at UAH

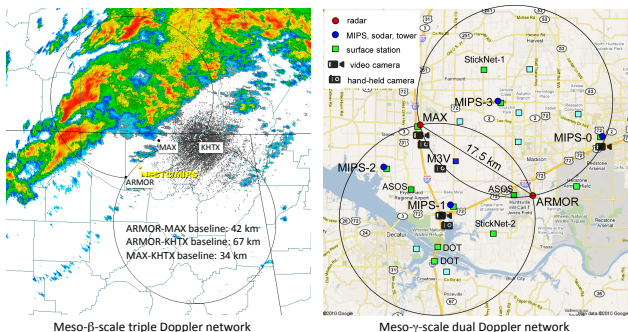
Kevin Knupp and Larry Carey

ARMOR: Advanced Radar for Meteorological and Operational Research (fixed)

Freq: 5625 MHz
 λ : 5.3 cm
 Polarization: H,V (STAR)

PRF: 250-2000 Hz
 Pulse length: 0.4-2.0 ms
 Xmit: Magnetron, 350 kW

Antenna diam: 3.7 m
 Beamwidth: 1.0°
 Signal Proc: RVP-8



MAX: Mobile Alabama X-band

Freq: 9450 MHz
 λ : 3.2 cm
 Polarization: H,V (STAR)

PRF: 250-2000 Hz
 Pulse length: 0.4-2.0 μ s
 Xmit: Magnetron, 250 kW

Antenna diam: 2.4 m
 Beamwidth: 0.95°
 Signal Proc: RVP-8



MAX deployed at the New Market site 42 km NE of the ARMOR

MIPS: Mobile Integrated Profiling System



Doppler wind profiler (915)

Freq: 915 MHz
 λ : 32.8 cm
 Polarization: single

PRF: variable
 Pulse length: 0.4-2.0 μ s
 Xmit: Solid state, 500 W

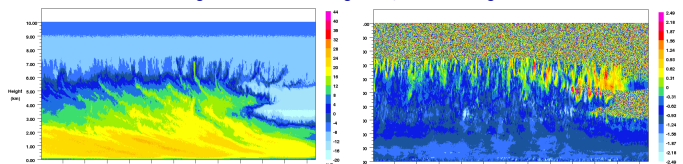
Antenna diam: 2 m
 Beamwidth: 9°
 Signal Proc: digital

X-band Profiling Radar (XPR)

Freq: 9410 MHz
 λ : 3.2 cm
 Polarization: single

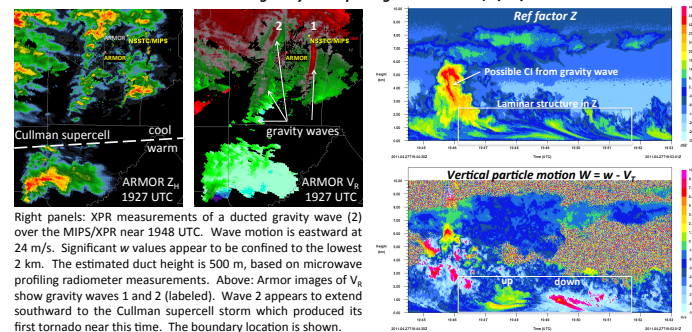
PRF: 1000-2000 Hz
 Pulse length: 0.2-1.0 μ s
 Xmit: Magnetron, 25 kW

Antenna diam: 1.8 m
 Beamwidth: 1.2°
 Signal Proc: Gamic

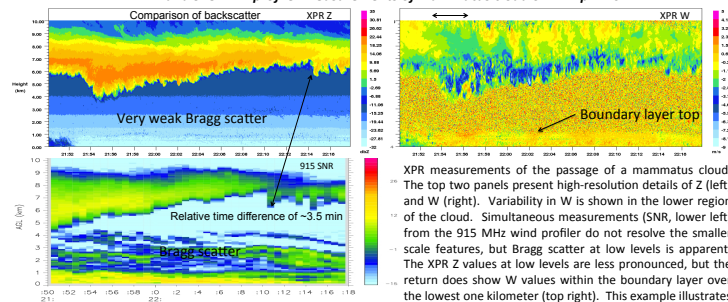


One of the first set of XPR measurements during the Profiling of Winter Storms (PLOWs) project on 14 February 2010. These two images show the fine structural details of convective elements near cloud top (7 km AGL). This was a common feature measured in even greater detail by the Wyoming Cloud Radar on the NCAR WC-130, which was conducting linear flight legs at multiple altitudes along a line over the MIPS, MAX and NCAR MISS platforms over southern Indiana.

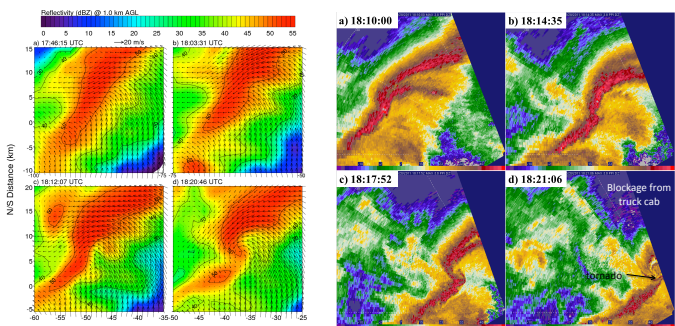
Second ducted gravity wave passage over the XPR, 4/27/11



XPR and 915 MHz profiler measurements of mammatus cloud on 21 April 2011

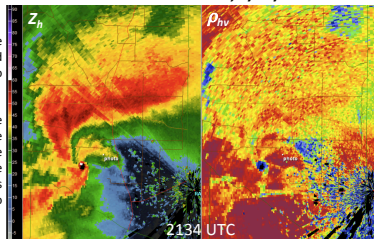


XPR measurements of the passage of a mammatus cloud. The top two panels present high-resolution details of Z (left) and W (right). Variability in W is shown in the lower region of the cloud. Simultaneous measurements (SNR, lower left) from the 915 MHz wind profiler do not resolve the smaller scale features, but Bragg scatter at low levels is apparent. The XPR Z values at low levels are less pronounced, but the return does show W values within the boundary layer over the lowest one kilometer (top right). This example illustrates the ability to identify Bragg vs. Rayleigh scatter.



Tornado genesis with a QLCS on 28 February 2011. The left panel shows the dual Doppler analysis (ARMOR/KHTX) of storm-relative airflow at 1 km AGL. The increase in vorticity within the mesocyclone coincided with the passage of a quasi-linear reflectivity feature (QLRF) with the storm core. The right panels show higher resolution details of Z from MAX between 1810 and 1821 UTC. Panel d shows a tornado signature 6 km NNW of the MAX radar.

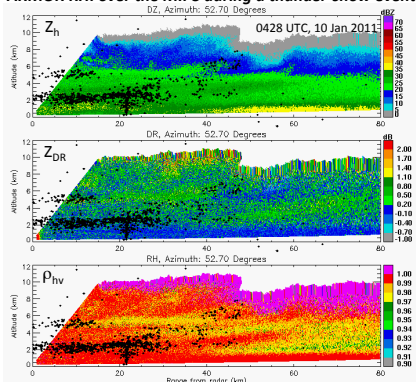
Tornado outbreak, 4/27/11



Top right: ARMOR 0.7° PPI showing the Hackleburg storm near a point of high-end EF-4 damage at 2134 UTC. The tornado location is circled in both panels.

Bottom right: Close-up view of Z_h from the KHTX, ARMOR, and MAX radars within the midday tornadic QLCS. Tornado tracks are represented by the white lines. The circulation indicated by the Z patterns produced multiple, closely-spaced EF-0 to EF-1 tornadoes.

ARMOR RHI over the MIPS during a thunder-snow event



All UAH assets were deployed during a thunder-snow event over northern Alabama on 10 January 2011. Frequent RHI scans were conducted over the MIPS, located at 52.7 deg, 14 km from the ARMOR. These images show VHF sources (black dots) detected by the lightning mapping array superimposed on the vertical plane of the RHI images. Layering of sources indicates long horizontal channels near 2 km AGL (and secondarily at 5 km) and a CG lightning strike near a range of 22 km (tower induced). Liquid water detected by the microwave profiling radiometer was present within the lowest 2 km.

